

Detachment of nanotubes from a polymer matrix

Carole A. Cooper

Department of Materials and Interfaces, Weizmann Institute of Science, P.O.B. 26, Rehovot 76100, Israel

Sidney R. Cohen

Chemical Services Unit, Weizmann Institute of Science, P.O.B. 26, Rehovot 76100, Israel

Asa H. Barber and H. Daniel Wagner^{a)}

Department of Materials and Interfaces, Weizmann Institute of Science, P.O.B. 26, Rehovot 76100, Israel

(Received 7 May 2002; accepted 20 September 2002)

A technique to investigate the adhesion of carbon nanotubes to a polymer matrix is described. Carbon nanotubes bridging across holes in an epoxy matrix have been drawn out using the tip of a scanning probe microscope while recording the forces involved. A full force-displacement trace could be recorded and correlated with transmission electron micrographs observations prior and subsequent to the tip action. Based on these experiments, an approximate calculation of the nanotube-polymer interfacial shear strength has been performed. © 2002 American Institute of Physics. [DOI: 10.1063/1.1521585]

The remarkable physical properties of carbon nanotubes are currently stimulating the imagination of scientists in various disciplines. Extensive work, described in recent articles¹ has led to significant success in the measurement of their mechanical properties. The strength of nanotube-reinforced polymers is studied much less. Conjectural or computer-simulated results suggest that the nanotube-polymer adhesion may in some cases attain high values—up to hundreds of megapascal under certain conditions^{2–4}—thus an order of magnitude higher than the stress transfer ability of current advanced fiber-based composites. The question of strength of the polymer-nanotube interface remains speculative due to the paucity of studies on nanotube-polymer adhesion.^{2–7} Single-walled carbon nanotube (SWNT)/polymer nanocomposites containing holes spanned by well-anchored bundles of SWNTs were previously prepared in our laboratory.⁸ Such samples provide an excellent opportunity to measure the adhesion of individual carbon nanotubes to a polymer matrix. In this report the nanotube-polymer interaction was quantified by detaching individual SWNT bundles and multiwalled-carbon nanotube (MWNTs) from an epoxy matrix using a scanning probe microscope (SPM) tip. Location of suitable polymer holes and nanotubes and imaging of their subsequent detachment was achieved by transmission electron microscopy (TEM). The present experiment represents the first attempt to directly measure the interfacial adhesion in nanocomposites.

The matrix used for the nanocomposite was an epoxy resin (Araldite LY564, Ciba-Geigy, hardener HY560). The MWNTs (diameter range: 10–15 nm; length range: 2–3 μm) were obtained from Dynamic Enterprises Ltd, UK, and the SWNTs (diameter range: 1.4–2 nm; length ~1 μm) were purchased from Tubes@Rice, Texas. The nanotubes were dispersed in the epoxy resin (3 wt %) using a high intensity ultrasonic processor. The hardener was then added and me-

chanically mixed with the epoxy/nanotube mixture. Approximately 200-μm-thick films were prepared, left at room temperature for 24 h and then cured at 72 °C for 3 h followed by slow cooling back to room temperature. The final composite specimens were microtomed into thin (70–100 nm) films parallel to the film surface using a diamond knife (Micro Star Co.) and a Reichert–Jung ultracut microtome (at room temperature), and then transferred to a labeled TEM grid upon which both TEM and SPM measurements were made. The TEM employed was a Philips CM120 at 120 kV. For the SPM measurements, the grid was placed on a 50-μm-thick Kapton 200HN sheet (DuPont) with the sample sandwiched between sheet and grid. The SPM measurements were made on an NT-MDT P7-LS system equipped with high-power optical microscope (Navitar 12×zoom). SPM imaging was performed in the semicontact mode in order to locate the region of interest and position the tip in the appropriate place. The pullout step was accomplished in contact mode by sliding the tip across the hole spanned by the nanotube (motion perpendicular to the cantilever long axis and intersecting the nanotube axis), while monitoring lateral force and position with a digital scope (Nicolet 400). The pullout force and work could then be calculated from the scope trace.

A variety of phenomena were observed, including nanotube pullout (partial or complete), bending or breakage of nanotubes, and unsheathing of inner from outer tube layers. In some cases, the polymer matrix was damaged, so that it was not always possible to assign the measured shear strengths to the pullout alone. In such cases, the value derived would represent an upper bound for the shear strength. The force acting on a nanotube as a result of pulling out with the SPM tip (along the scan direction) was not normal to the nanotube axis, therefore the lateral force was resolved into its component parallel to the relevant direction (along the tube axis for pullout, and perpendicular to it for breakage). Examination of the force traces indicates that bending of the nanotube before pullout was small, typically <6°, so that no additional force resolution was required at the embedded NT-free NT interface.

^{a)}Author to whom correspondence should be addressed; electronic mail: daniel.wagner@Weizmann.ac.il

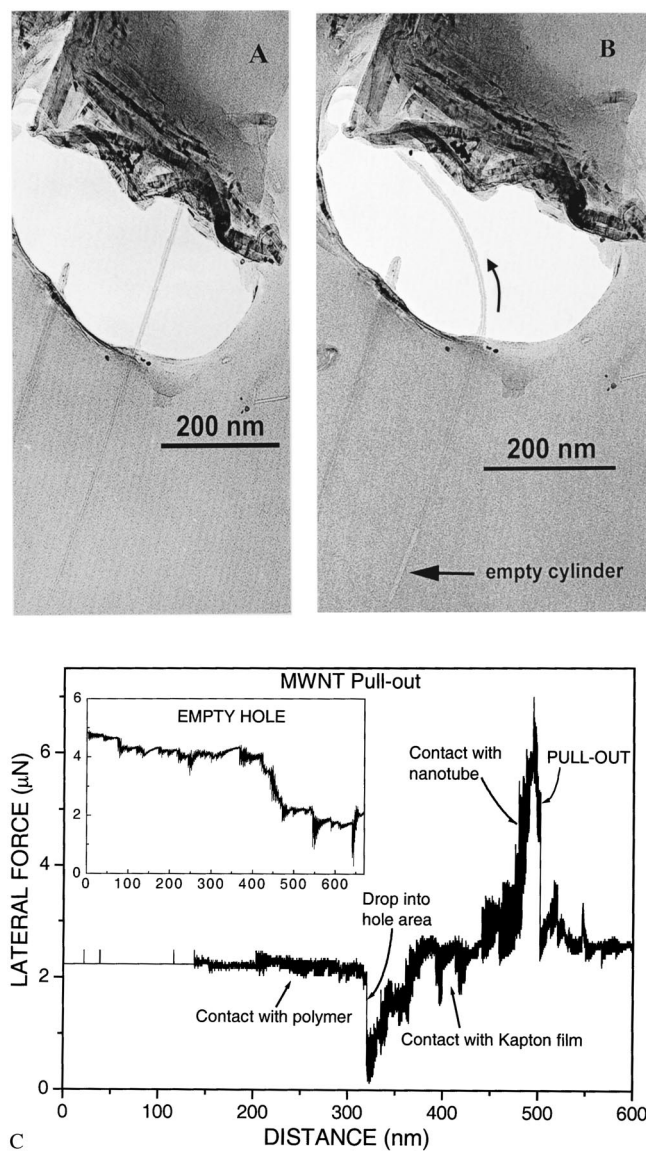


FIG. 1. TEM images of a MWNT crossing a hole in an epoxy resin matrix. (a) TEM image of nanotube bridging matrix hole. The bridging nanotube in these images has a diameter of 8.2 nm. (b) TEM image of same specimen following partial pullout by means of a SPM tip. The larger arrow shows the direction of the tip movement; the small arrow indicates the empty cylindrical hole left behind after partial pullout. (c) Force-distance curve obtained for this specimen shows the dependence of the lateral force on distance traveled by the SPM tip. The force-distance curve for an empty hole scanned by the SPM tip is also shown on the same plot.

Figure 1(a) shows a TEM micrograph of a MWNT spanning a polymer cavity. After dragging across the hole with the SPM tip, it could be seen [Fig. 1(b)] that the MWNT had been fully pulled out from the top of the hole and partially drawn out of the bottom of the hole leaving a cylindrical cavity, as a result of loading the nanotube at its center (analogous to a cable with two fixed ends and a center loading). The nanotube is bent in the direction of the pull. The corresponding force-distance ($F-d$) curve is shown [Fig. 1(c)], with the pullout event assigned to the peak in the curve. The $F-d$ trace resembles a typical stress versus displacement curve for fiber pullout tests.^{9–11} The $F-d$ trace describes the path of the SPM tip across the matrix hole and suspended MWNT. The trace line dips as the SPM tip drops into the hole, due to changing friction of the tip against a different substrate. The force then increases steadily as the tip connects with the nanotube and is followed by a sharp drop as the tip draws the nanotube out of the polymer. The inset shows the $F-d$ curve for an empty polymer hole also scanned by the SPM tip whereby the sharp peak that was observed for all of the nanotube pullouts is absent. The embedded MWNT length can be deduced by comparing the observed embedded and free length plus the length of the empty cylinder observed in Fig. 1(b). The bending force,¹² calculated from the deflection arm (120 nm), radius (4.1 nm), bending stiffness (1.2 TPa¹³) and deflection (220 nm) is 0.1 μ N, which is insignificant relative to the 3.8 μ N angularly resolved pullout force. The shear strength for the MWNT was calculated by dividing this pullout force by the interfacial area of the embedded nanotube. The nanotube dimensions, work and pullout energy, and shear strength calculations for the pullout specimens are presented in Table I. It is likely that some of the energy measured during pullout was related to stretching the polymer film. This may lead to an overestimate in the energy, but not in the maximum force.

SWNTs predominantly bundled together in ropes that spanned the polymer voids. Of all the SWNT specimens tested, only one (specimen 7, Table I) could be pulled out, the rest undergoing fracture. Hence, as the ropes had fractured, the rope strength rather than an interfacial shear strength was calculated, as presented in Table II. In these cases, the force required to pull these tubes out must be even higher than that required to break them. Calculations of the

TABLE I. Experimental data for nanotube pullout. Note: Errors contributing to the shear strength calculations included the measurement of the interfacial area (consisting of the nanotube diameter and especially the embedded length, which was sometimes partially concealed, leading to inflated values of the interfacial adhesion) and the fractional components of the lateral force signal, which were directed along the pullout direction.

Specimen	MWNT						SWNT rope
	1	2	3	4	5	6	
Diameter (nm)	8.2	11.0	24.0	13.4	13.4	24	11.6
Embedded length (nm)	484	256	2570	379	708	1870	193
Interfacial area ($m^2 \times 10^{-14}$)	1.01	0.88	19.4	1.60	2.99	14.07	0.71
Max. force (μ N)	3.8 ± 0.5	2.8 ± 0.6	6.8 ± 1.7	0.6 ± 0.04	2.3 ± 0.6	12.8 ± 2.1	2.6 ± 0.5
Work ($J \times 10^{-13}$)	2.9	3.3	16	1.3	1.6	7.8	4.1
Pullout energy ($J m^2$)	26.4	36.9	8.2	0.9	5.35	5.54	25.6
Shear strength (MPa)	376 ± 40	318 ± 16	35 ± 9	38 ± 2	77 ± 20	91 ± 15	366 ± 74

TABLE II. Experimental data for SWNT rope breaking. Note: A_{all} =cross-sectional area calculated for all nanotubes in a SWNTs rope; A_{perim} =cross-sectional area calculated from the peripheral nanotubes only; σ_{all} calculated assuming all nanotubes are carrying load and σ_{perim} assuming just the perimeter nanotubes are carrying the load.

	SWNT ropes		
Specimen	6	7	8
Diameter (nm)	15.6	16.2	11.5
Embedded length (nm)	568	1603	709
Cross-sectional area ($\text{m}^2 \times 10^{-17}$)	A_{all} 11.1	A_{perim} 4.32	14.4 5.04
Max Force (μN)	30.7 \pm 5.5	6.0 \pm 0.7	5.0 \pm 2.2
Work ($\text{J} \times 10^{-13}$)	14.6	9.6	1.6
Breaking strength (GPa)	σ_{all} 277 \pm 50	σ_{perim} 711 \pm 127	42 \pm 5 114 \pm 50
			236 \pm 103

breaking strength assumed that the rope cross sections are round in shape.¹⁴ If all SWNT in a rope are assumed to carry an equal load, the relevant cross section is obtained by multiplying the cross section of one nanotube (wall thickness 0.34 nm) by the total number of tubes in the rope. Alternatively, we also present the strength obtained by assuming that only the perimeter nanotubes carry the load.¹⁴ SWNT bundles tested under tensile loading by Yu *et al.*¹⁴ resulted in the average breaking strength of 30 GPa assuming that the load is carried by the SWNTs on the perimeter of each bundle. Our experiment is not a true tensile loading since the stress is applied laterally. Further, the SWNT ropes are firmly embedded in the polymer matrix as indicated by good wetting seen in the TEM micrographs (not shown). Thus, fracture would be a complex process involving rupture of the polymer-nanotube interface coupled with bending of the rope. These additional modes for energy dissipation could lead to high fracture strengths.

A correlation between interfacial shear strength and embedded length (l_e) is presented in Fig. 2. The interfacial shear strength falls with increasing l_e , reminiscent of the falloff seen in single-fiber pullout tests due to an “ineffective length” over which most of the shear stress transfer occurs.⁹

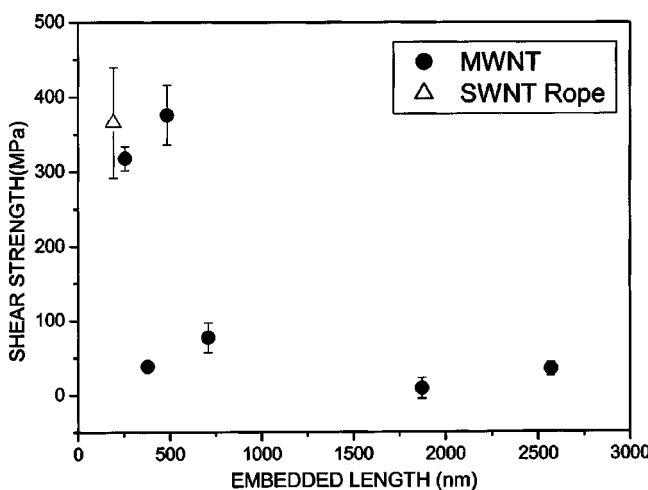


FIG. 2. Correlation between shear strength and embedded nanotube length.

Our measurements support the prediction^{2–4,7} that the nanotube-polymer interface strength can be significantly higher than similar measurements in fiber-polymer interfaces. This apparent capability of the nanotube polymer interface to sustain more shear than the matrix could be due to one of several reasons: Molecular dynamics simulations show that the existence of covalent bonding between nanotube and polymer could lead to shear strengths on the order of those measured here.⁷ Such bonding could arise from naturally occurring defect sites at the NT wall, and those arising from interaction with the electron beam in the TEM.¹⁵ The mechanical behavior the ultrathin polymer layer at the interface may be different than that of bulk polymers. A generalized Kelly-Tyson scheme predicts interfacial strengths of hundreds of megapascal under certain conditions, albeit with high variability due to the presence of defects in the SWNT structure.⁴ Indeed, significant specimen to specimen data variability was observed. Conversely, point defects leading to covalent NT-polymer bonding would strengthen the interface, the nonstatistical presence of such defects also leading to variable results.

An experimental technique for probing individual carbon nanotube pullout from a polymer matrix has been presented. The procedure provides a direct measurement of the shear strength of the carbon nanotube/polymer interface for MWNT specimens. Only one SWNT rope specimen underwent pullout, with most experiments resulting in SWNT rope fracture. In these cases, the SWNT-polymer adhesion must exceed SWNT rope strength. The high values of interfacial strength and breaking strength measured here indicate that in some cases, substantial adhesion exists between the nanotubes and the epoxy resin matrix.

This project was supported by the (CNT) Thematic European network on “Carbon Nanotubes for Future Industrial Composites” (EU), the G. M. J. Schmidt Minerva Center of Supramolecular Architectures, and by the Israel Science Foundation. H.D.W. is the recipient of the Livio Norzi Professorial Chair.

- 1 E. T. Thostenson, Z. Ren, and T.-W. Chou, Compos. Sci. Technol. **61**, 1899 (2001), and references therein.
- 2 H. D. Wagner, O. Lourie, Y. Feldman, and R. Tenne, Appl. Phys. Lett. **72**, 188 (1998).
- 3 K. Liao and S. Li, Appl. Phys. Lett. **79**, 4225 (2001).
- 4 H. D. Wagner, Chem. Phys. Lett. **361**, 57 (2002).
- 5 L. S. Schadler, S. C. Giannaris, and P. M. Ajayan, Appl. Phys. Lett. **73**, 3842 (1998).
- 6 O. Lourie and H. D. Wagner, Compos. Sci. Technol. **59**, 975 (1999).
- 7 S. J. V. Frankland, A. Caglar, D. W. Brenner, and M. Griebel, J. Phys. Chem. B **106**, 3046 (2002).
- 8 O. Lourie and H. D. Wagner, Appl. Phys. Lett. **73**, 3527 (1998).
- 9 M. J. Pitkethly and J. B. Doble, Composites **21**, 389 (1990).
- 10 Z.-F. Li and D. T. Grubb, J. Mater. Sci. **29**, 189 (1994).
- 11 S. Y. Fu and B. Lauke, J. Adhes. Sci. Technol. **14**, 437 (2000).
- 12 E. W. Wong, P. E. Sheehan, and C. M. Lieber, Science **277**, 1971 (1997).
- 13 Z. I. Wang, R. P. Gao, Z. W. Pan, and Z. R. Dai, Adv. Eng. Mats. **3**, 657 (2001).
- 14 M.-F. Yu, B. S. Files, S. Arepalli, and R. S. Ruoff, Phys. Rev. Lett. **84**, 5552 (2000).
- 15 M. Terrones, J. Banhart, N. Grobert, J.-C. Charlier, H. Terrones, and P. M. Ajayan, Phys. Rev. Lett. **89**, 075505 (2002).